f Element croconates
1. Lanthanide croconates — synthesis, crystal structure and thermal behaviour

Chantal Brouca-Cabarrecq and Jean-Christian Trombe*
CEMES-LOE/CNRS, 29 rue Jeanne Marvig, B.P. 4347, 31055 Toulouse Cédex (France)

(Received July 2, 1991; revised September 25, 1991)

Abstract

Lanthanide croconates free of alkaline elements have been prepared by using croconic acid or triethanolammonium croconate. They are divided into two families: **1**-Ln: $[Ln(H_2O)_5]_2(C_5O_5)_3 \cdot 4H_2O$ with Ln(III) = Ce, Pr, Nd, Sm, Eu, Gd; **2**-Ln: $[Ln(H_2O)_6]_2(C_5O_5)_3 \cdot 3H_2O$ with Ln(III) = Tb, Dy, Ho, Er, Yb. In the general conditions used to synthesize such complexes, lanthanum, lutetium and yttrium belong neither to the family **1**-Ln nor to the family **2**-Ln. In the presence of oxygen and exposed to daylight the latter elements induce, after a few days, a degradation of the croconate ligand leading to oxalate complexes and to another phase still unknown. A possible hypothesis is presented. A structural study has been performed on a single-crystal representative on each family: Pr for **1**-Ln, Er for **2**-Ln. The first family crystallizes in the orthorhombic system, space group *Pccn*, while the second one crystallizes in the triclinic system, space group *P*1. The salient feature of both structures consists of discrete, neutral, dinuclear entities: $[Ln(H_2O)_x]_2(C_5O_5)_3$, with $x = 5$ for **1**-Ln and $x = 6$ for **2**-Ln. However, these entities differ markedly from one family to the other by the coordination mode of the croconate ligand. For **1**-Ln the two independent croconates are either chelating or bis-chelating while for **2**-Ln the three independent croconates are monodentate and transmonodentate. Between the two structures, a modification of the lanthanide coordination number takes place: 9 for Pr as a distorted trigonal tricapped prism, 8 for Er (Er1 and Er2) as a deformed antisquare prism. The crystal structure is assured, in both cases, by hydrogen bonding and van der Waals interactions between stacked croconate planes. Free water molecules are localized in tunnels. Dehydration of lanthanide croconates of each family takes place in a single step around 90 to 150 °C; anhydrous compounds are stable. The decomposition of the croconate ligand proceeds via oxycarbonate according to the considered lanthanide. It starts around 310 °C, and constant weight is achieved at a variable temperature up to 700 °C, leading to the corresponding oxides. An endotherm is found for the dehydration, a strong exotherm for the croconate decomposition.

Introduction

A croconate ligand is a member of the delocalized π-bond cyclic oxocarbon family which contains deltate, squarate, croconate and rhodizonate members [1]. The discovery of croconic acid dates from Gmelin in 1825 [2], however this ligand has been the object of few studies as compared to the squarate one. In the period 1950–1965 the work of West and Niu on oxocarbon chemistry was rather from an organic point of view [1, 3]. During the same period, a croconate synthesis was proposed [4] and some structural works (NH_4^+, Mn^{2+}, Cu^{2+}, Zn^{2+}) were performed [5–8]. In the three latter structures which are isostructural, the croconate ligand appears to be in the 1,2,4-coordination mode (1,2-chelation). Only recently have other articles dealing with croconate acting as a chelating ligand appeared [9–11].

For more than ten years our research has been focused on the structure–physicochemical properties relationships in low dimensional complexes. Such compounds, either homo or heterometallic, are built around small ligands such as dithiooxalates [12–15], squarates [16] or dithiosquarates [16]. Our interest now includes the croconate ligand. In a previous paper, the synthesis and structural determination of a cerium–potassium croconate, $CeK(H_2O)_7(C_5O_5)_2$, was described: this phase is isostructural with the sodium one [17, 18]. Neutral, illimited, ordered, bimetallic chains are formed. The chelation mode is realized towards the alkaline element, but an oxygen atom inside the bite is also bound to a cerium atom.

Cerium behaviour in sodium or potassium croconate solution has been extended to the whole lanthanide

*Author to whom correspondence should be addressed.

0020-1693/92/$5.00

series. According to EDAX analyses two phases were obtained: both these phases contained the lanthanide element but they differed as to the presence of the alkaline one. Besides, during lanthanide contraction the proportion of these two phases varied: the bulkier was the lanthanide element [19] the higher was the proportion of the bimetallic phase [17, 20]. Only for the cerium element, was the bimetallic phase analytically pure.

Our main goal was to obtain lanthanide croconates free from an alkaline element. In this paper, the way of synthesizing such complexes, which are divided into two families, is described as well as the thermal behaviour of these compounds. A crystal structure determination of a complex representative of each family has been realized. Only one paper dealing with lanthanide croconates has been reported in the literature [21]; it deals with the thermodynamical parameters of such complexes in solution.

Experimental

Synthesis

Potassium croconate as well as barium croconate were prepared according to the literature method [4]. To avoid the presence of potassium a cation exchange resin loaded either in H^+ or in $(C_2H_5OH)_3NH^+$ was used. At the end of the resin the resulting solution was dropped into a lanthanide chloride solution. Another method consisted in refluxing a faint excess of lanthanide sulfate solution over barium croconate: barium sulfate precipitated and was filtered off, then the solution was cooled. Sometimes the latter method failed: instead of obtaining the lanthanide croconate, lanthanide sulfate was recovered. Indeed lanthanide sulfates are known to be faintly soluble and this solubility is variable along the lanthanide series. The two former methods (exchange-resin) which differed by their pH (croconic acid pH $\approx$ 1.5, triethanolammonium croconate pH $\approx$ 3–4) led to the same compounds. However a preference will be given to the use of triethanolammonium croconate because of the presence of well developed single crystals.

A typical experiment started with 0.5 mmol of croconate anion and 0.75 mmol of lanthanide salt in aqueous medium (20 ml). After a few days, generally less than a week, micro-crystals appeared, which were filtered, washed with a minimum amount of distilled water and air dried.

Characterization

According to X-ray powder diffraction the lanthanide croconates are distributed into two families according to the size of the considered lanthanide: **1**-Ln: $[Ln(H_2O)_5]_2(C_5O_5)_3 \cdot 4H_2O$ with Ln = Ce, Pr, Nd, Sm, Eu, Gd; **2**-Ln: $[Ln(H_2O)_6]_2(C_5O_5)_3 \cdot 3H_2O$ with Ln = Tb, Dy, Ho, Er, Yb. These formulae are deduced from the structure determination. It is noteworthy that some lanthanide elements, lanthanum, lutetium, yttrium (through the yttrium element is not strictly speaking a lanthanide) are not ranged into these families, they require special conditions (see 'discussion'). Elemental analyses (lanthanide, carbon, hydrogen) carried out by the Laboratoire Central de Microanalyse du CNRS are reported in Table 1; they agree rather well with those calculated from the above formulae.

TABLE 1. Elemental analysis (%) for the compounds of the **1**-Ln and **2**-Ln families

	1-Ln					
	Ce	Pr	Nd	Sm	Eu	Gd
Calculated						
Ln	29.42	29.56	30.03	30.91	31.15	31.88
C	18.90	18.87	18.74	18.50	18.44	18.25
H	2.94	2.93	2.91	2.88	2.87	2.84
Observed						
Ln	29.9	29.2	29.7	29.2	31.2	31.1
C	19.2	19.3	19.1	18.9	19.0	18.5
H	3.0	3.0	3.1	3.1	2.8	2.9
	2-Ln					
	Tb	Dy	Ho	Er	Yb	
Calculated						
Ln	31.54	32.02	32.34	32.65	33.40	
C	17.86	17.73	17.65	17.57	17.37	
H	2.98	2.96	2.94	2.93	2.89	
Observed						
Ln	31.6	31.3	32.1	32.3	33.4	
C	18.3	18.4	17.7	17.8	17.4	
H	2.8	2.4	2.8	2.6	2.8	

IR spectra (KBr pellets) were performed. Whatever the compound or family, they exhibit bands in the field characteristic of the croconate ligand or of water molecules. In particular the bands at about 1680 and 1720 cm^{-1} show that the C–O bond retains a considerable double bond character [5].

Thermal analyses (oxygenated atmosphere, heating rate 5 °C/mn) were carried out on a Setaram B85 microbalance and Setaram M5 microanalyser with Al_2O_3 as reference.

Crystal structure determination

Single crystals of **1**-Pr, representative of the first family, and **2**-Er representative of the second family were mounted on a CAD-4 Enraf-Nonius diffractometer.

Orientation matrices and accurate cell constants were derived from least-squares refinements of the setting angles of 25 reflections. Crystal data and conditions of intensity measurements are reported in Table 2. The standard reflections showed no abnormal trend. The data were corrected for Lorentz and polarization effects, and absorption corrections were applied [22].

Structure determinations were carried out using Patterson and Fourier map techniques and refined applying full-matrix least-squares techniques on a DEC VAC 11-730 computer using programs listed in ref. 23. Throughout the refinements, the minimized functions were $\Sigma w(|F_o| - |F_c|)^2$ where $|F_o|$ and $|F_c|$ are the observed and calculated structure factor amplitudes. Atomic scattering factors and anomalous terms are those of Cromer and Waber [24]. Weighting schemes and reliability factors are reported in Table 2. The H atoms which were located from difference Fourier maps were introduced in the last cycles of refinement as fixed contributors with isotropic thermal parameters.

TABLE 2. Experimental crystallographic data for $[Pr(H_2O)_5]_2(C_5O_5)_3 \cdot 4H_2O$ (family **1**-Ln) and $[Er(H_2O)_6]_2(C_5O_5)_3 \cdot 3H_2O$ (family **2**-Ln)

	PrCR	ErCR
Crystal data		
Crystal system	orthorhombic	triclinic
Space group	*Pccn*	*P*1
a (Å)	10.922(1)	9.221(1)
b (Å)	17.397(3)	9.602(2)
c (Å)	15.742(2)	8.591(1)
α (°)		94.58(1)
β (°)		97.67(1)
γ (°)		93.81(1)
V (Å^3)	2991.2	749.1
Z	4	1
Molecular weight (g)	954.2	1024.5
ρ_{calc} (g/cm^3)	2.12	2.27
μ(Mo Kα) (cm^{-1})	33.15	57.145
Morphology	truncated pyramid with hexagonal base	parallelipiped
Dimension (mm)	0.3×0.2×0.2×0.2	0.04×0.03×0.015
Transmission coefficient: min., max.	77.4, 100.0	87.5, 100.0
Data collection		
Temperature (K)	293	293
Wavelength (Mo Kα) (Å)	0.71073	0.71073
Monochromator	graphite	graphite
Scan mode	$\omega-2\theta$	$\omega-2\theta$
Scan width (°)	0.80+0.35 tgθ	1.10+0.35 tgθ
Take-off angle (°)	3.8	5.5
Max. Bragg angle (°)	30	30
Scan speed[a]		
SIGPRE[a]	0.66	0.75
SIGMA[a]	0.018	0.018
VPRE (°/min)[a]	10	10
T_{max}(S)[a]	70	60
Intensity control reflections (every 3600 s)	0 6 2/3 2 5/5 5 5	2 −1 1/3 3 3/2 −3 1
Orientation control reflections (every 100 reflections)	20 0 0/0 22 0/−8 −12 −8	0 0 8/8 0 0/0 −9 0
Attenuation factor	19.4	19.4
Structure refinement		
Reflections collected	6713	4160
Reflections used	3977 ($I>3\sigma(I)$)	3902 ($I>2\sigma(I)$)
No. refined parameters	204	417
Weighting, w^{-1}	$\sigma^2(F_o)+(0.01F_o)^2+1$	$\sigma^2(F_o)+F_o^2$
$R=\Sigma\|\|F_o\|-\|F_c\|\|/\Sigma\|F_o\|$	0.034	0.038
$R_w=[\Sigma w(\|F_o\|-\|F_c\|)^2/\Sigma wF_o^2]^{1/2}$	0.038	0.044

[a]For definition of parameters see ref. 25.

1-Ln: $[Pr(H_2O)_5]_2(C_5O_5)_3 \cdot 4H_2O$

Praseodymium croconate crystallizes in the orthorhombic system. The systematic absences of reflections $0kl$ with $l=2n+1$, $h0l$ with $l=2n+1$ and $hk0$ with $h+k=2n+1$ were consistent with space group *Pccn*. The eight expected Pr atoms, eight croconate cycles (CR1) and five water molecules bound to the Pr atom are on general positions. The remaining croconate (CR2), one-half per assymmetric unit, is symmetric with respect to the twofold axis: O32 and C32 are in special position 4d on the axis. Three crystallographic sites Ow6, Ow7, Ow8 are occupied by free water molecules, the latter two being partially occupied (50%). Hydrogen atoms of the water molecules (Ow1, Ow2, Ow3, Ow4, Ow5) coordinated to the Pr atom are found. In the last cycle of refinement the largest (variable shift)/(e.s.d.) ratio is 0.06 and the reliability factors converge at $R=0.034$, $R_w=0.038$ for 3977 observations ($I>3\sigma(I)$) and 204 variables (Table 2). The error in an observation of unit weight is 0.96 e^-. The final difference Fourier map does not give significant features. The final parameters with their e.s.d.s are given in Table 3.

2-Ln: $[Er(H_2O)_6]_2(C_5O_5)_3 \cdot 3H_2O$

Erbium croconate crystallizes in the triclinic system. By using the centrosymmetric spatial group, the position of erbium was determined from a three-dimensional Patterson. The first croconate cycle CR1 is found easily, as well as five water molecules bound to the erbium atom. The missing croconate CR2, one half per asymmetric unit, can be located on a subsequent difference Fourier map; O22 is in a special position $(\frac{1}{2}, \frac{1}{2}, \frac{1}{2})$ having crystallographically point symmetry of -1, so that the CR2 cycle appears to be disordered through the O22 atom. The site occupation of each atom belonging to the croconate CR2 could be not higher than 0.5, that is found for all atoms except O12 and O32 having 100% occupancy. These sites could be 50% occupied by these atoms and 50% by water molecules. Although the structure results were good enough using $P\bar{1}$, the refinement was started again using the non-centrosymmetric group. The positions of the erbium atom in the centrosymmetric space group were affected to those of Er1 atom in the non-centrosymmetric group. A supplementary Er2, three croconates and twelve water molecules (six per erbium atom) were easily found. Four free water molecules were localized. The two latter water molecules have 50% site occupancy. Hydrogen atoms were found only for water molecules bound to the erbium atoms. In the last cycle of refinement the highest (variable shift)/(e.s.d.) is equal to 0.10 and the reliability factors stabilized at $R=0.038$, $R_w=0.044$ for 417 variables and 3902 observations having $I>2\sigma(I)$ (Table 2). The error in an observation of unit weight is 1.87 e^-. The absolute configuration is checked.

TABLE 3. Atomic positions and equivalent thermal parameters for $[Pr(H_2O)_5]_2(C_5O_5)_3 \cdot 4H_2O$ (family **1**-Ln)

Atom	*x*	*y*	*z*	*B* (Å²)[a]
Pr	0.48412(2)	0.09161(1)	0.30395(1)	2.672(3)
Ow(1)	0.2534(4)	0.0825(3)	0.3082(3)	6.5(1)
Ow(2)	0.4198(4)	−0.0416(2)	0.2691(2)	4.99(8)
Ow(3)	0.6667(3)	0.0155(3)	0.3486(2)	4.77(8)
Ow(4)	0.3916(4)	0.2202(2)	0.3313(3)	5.51(9)
Ow(5)	0.4182(4)	0.0361(3)	0.4429(2)	5.40(9)
Ow(6)	0.4187(6)	−0.1691(4)	0.3708(4)	9.9(2)*
Ow(7)	0.1491(8)	0.1808(5)	0.1930(6)	5.5(2)*
Ow(8)	0.143(1)	0.1520(6)	0.0678(7)	7.0(2)*
O(11)	0.4036(3)	0.1425(2)	0.1651(2)	3.68(6)
O(21)	0.6014(3)	0.0425(2)	0.1724(2)	3.08(6)
O(31)	0.7047(3)	0.0232(2)	−0.0024(2)	3.97(7)
O(41)	0.5517(4)	0.1158(2)	−0.1157(2)	4.56(8)
O(51)	0.3728(4)	0.1975(3)	−0.0132(2)	5.80(9)
O(12)	0.6489(3)	0.1895(2)	0.2578(2)	3.96(7)
O(22)	0.5935(3)	0.1559(2)	0.4281(2)	3.87(7)
O(32)	3/4	1/4	0.5409(3)	4.7(1)
C(11)	0.4644(4)	0.1255(3)	0.1010(2)	2.81(7)
C(21)	0.5668(3)	0.0732(2)	0.1038(2)	2.39(6)
C(31)	0.6165(4)	0.0636(3)	0.0193(2)	2.71(7)
C(41)	0.5399(4)	0.1107(3)	−0.0384(2)	2.98(7)
C(51)	0.4477(4)	0.1515(3)	0.0134(3)	3.35(8)
C(12)	0.7021(4)	0.2211(3)	0.3188(3)	2.91(7)
C(22)	0.6730(4)	0.2038(3)	0.4071(3)	2.83(7)
C(32)	3/4	1/4	0.4627(4)	2.9(1)
H(11)	0.214	0.048	0.313	4.0*
H(21)	0.199	0.125	0.331	4.0*
H(12)	0.434	−0.059	0.216	4.0*
H(22)	0.396	−0.077	0.299	4.0*
H(13)	0.723	0.038	0.402	4.0*
H(23)	0.697	−0.017	0.308	4.0*
H(14)	0.439	0.247	0.299	4.0*
H(24)	0.386	0.253	0.384	4.0*
H(15)	0.338	0.003	0.451	4.0*
H(25)	0.394	0.074	0.485	4.0*

[a]Starred items: the corresponding atoms have been refined with isotropic thermal parameters.

No significant features appear in the final difference Fourier map. The atomic positional and equivalent or isotropic parameter are listed in Table 4.

Description of the structures

Both structures, **1**-Ln and **2**-Ln, have similarities and differences. They are both made of discrete, neutral, dinuclear entities $[Ln(H_2O)_x]_2(C_5O_5)_3$. The crystal structure arises from the hydrogen bonding or van der Waals interactions between the croconate oxygen atoms and water molecules linked to the lanthanide and also interactions of stacked croconate planes. Differences mainly appear about the coordination mode of the croconate ligands and also about the lanthanide coordination number.

TABLE 4. Atomic positions and equivalent thermal parameters for $[Er(H_2O)_6]_2(C_5O_5)_3 \cdot 3H_2O$ (family **2**-Ln

Atom	x	y	z	B (Å²)[a]
Er(1)	0.264	0.220	0.174	1.79(1)
Ow(11)	0.077(1)	0.338(1)	0.044(1)	3.34(7)
Ow(21)	0.159(1)	0.011(1)	0.023(1)	2.84(7)
Ow(31)	0.316(1)	0.248(1)	−0.078(1)	3.18(7)
Ow(41)	0.449(1)	0.061(1)	0.150(1)	2.86(7)
Ow(51)	0.358(1)	0.154(1)	0.425(1)	3.05(7)
Ow(61)	0.479(1)	0.371(1)	0.198(1)	3.97(7)
O(11)	0.067(1)	0.134(1)	0.282(1)	2.63(7)
O(21)	−0.249(1)	0.106(1)	0.233(1)	2.69(7)
O(31)	−0.354(1)	0.154(1)	0.546(1)	3.21(7)
O(41)	−0.097(1)	0.212(1)	0.779(1)	3.16(7)
O(51)	0.167(1)	0.215(1)	0.623(1)	3.14(7)
C(11)	−0.0142(8)	0.1417(7)	0.3904(9)	1.9(1)*
C(21)	−0.1754(8)	0.1304(7)	0.3666(9)	2.1(1)*
C(31)	−0.2248(8)	0.1732(7)	0.5175(9)	1.9(1)*
C(41)	−0.0941(8)	0.2109(7)	0.6347(9)	1.8(1)*
C(51)	0.0360(8)	0.1915(7)	0.5561(9)	1.8(1)*
Er(2)	0.73637(6)	0.78029(6)	0.82593(6)	1.99(2)
Ow(12)	0.938(1)	0.677(1)	0.953(1)	3.09(7)
Ow(22)	0.846(1)	0.982(1)	0.973(1)	3.01(7)
Ow(32)	0.685(1)	0.735(1)	1.082(1)	3.05(7)
Ow(42)	0.552(1)	0.924(1)	0.860(1)	3.06(7)
Ow(52)	0.646(1)	0.821(1)	0.580(1)	2.73(7)
Ow(62)	0.772(1)	0.570(1)	0.686(1)	3.37(7)
O(12)	0.943(1)	0.866(1)	0.714(1)	2.63(7)
O(22)	1.263(1)	0.918(1)	0.757(1)	2.63(7)
O(32)	1.3613(9)	0.814(1)	0.459(1)	2.62(7)
O(42)	1.108(1)	0.755(1)	0.225(1)	2.70(7)
O(52)	0.847(1)	0.800(1)	0.376(1)	2.84(7)
C(12)	1.0208(8)	0.8472(7)	0.6102(9)	1.5(1)*
C(22)	1.1818(8)	0.8645(7)	0.6369(9)	2.0(1)*
C(32)	1.2343(8)	0.8438(7)	0.4833(9)	2.2(1)*
C(42)	1.1057(8)	0.8137(7)	0.3617(9)	1.8(1)*
C(52)	0.9737(8)	0.8159(7)	0.4402(9)	2.1(1)*
O(13)	0.2184(9)	0.4055(9)	0.3524(9)	2.72(7)
O(23)	0.520(1)	0.504(1)	0.491(1)	3.68(7)
O(33)	0.513(1)	0.645(1)	0.797(1)	3.59(7)
O(43)	0.2086(9)	0.6163(9)	0.865(1)	3.28(7)
O(53)	0.0259(9)	0.4946(9)	0.574(1)	3.40(7)
C(13)	0.261(1)	0.467(1)	0.487(1)	2.3(1)*
C(23)	0.410(1)	0.511(1)	0.555(1)	2.5(1)*
C(33)	0.405(1)	0.582(1)	0.711(1)	2.1(1)*
C(43)	0.250(1)	0.576(1)	0.743(1)	2.3(1)*
C(53)	0.161(1)	0.509(1)	0.600(1)	2.5(1)*
Ow(7)	0.611(1)	0.246(1)	0.886(1)	5.01(7)
Ow(8)	0.428(1)	0.793(1)	0.154(1)	4.81(7)
Ow(9)	0.899(1)	0.467(1)	0.249(1)	3.1(1)*
Ow(10)	0.681(1)	0.417(1)	0.032(1)	3.8(1)*
H(111)	0.010	0.289	−0.046	3.9*
H(211)	0.000	0.368	0.103	3.9*
H(121)	0.196	−0.022	−0.072	3.9*
H(221)	0.052	0.002	0.007	3.9*
H(131)	0.246	0.232	−0.174	3.9*
H(231)	0.411	0.226	−0.111	3.9*
H(141)	0.555	0.067	0.177	3.9*
H(241)	0.443	−0.041	0.118	3.9*
H(151)	0.464	0.152	0.461	3.9*
H(251)	0.304	0.189	0.507	3.9*
H(161)	0.519	0.418	0.301	3.9*

(continued)

TABLE 4. *(continued)*

Atom	*x*	*y*	*z*	*B* (Å²)[a]
H(261)	0.530	0.393	0.110	3.9*
H(112)	1.010	0.705	1.045	3.9*
H(212)	1.002	0.665	0.870	3.9*
H(122)	0.807	1.025	1.065	3.9*
H(222)	0.895	1.067	0.942	3.9*
H(132)	0.743	0.759	1.186	3.9*
H(232)	0.594	0.746	1.124	3.9*
H(142)	0.447	0.912	0.818	3.9*
H(242)	0.574	1.025	0.864	3.9*
H(152)	0.551	0.854	0.542	3.9*
H(252)	0.706	0.816	0.495	3.9*
H(162)	0.683	0.539	0.613	3.9*
H(262)	0.861	0.543	0.646	3.9*

[a]Starred items: the corresponding atoms have been refined with isotropic thermal parameters.

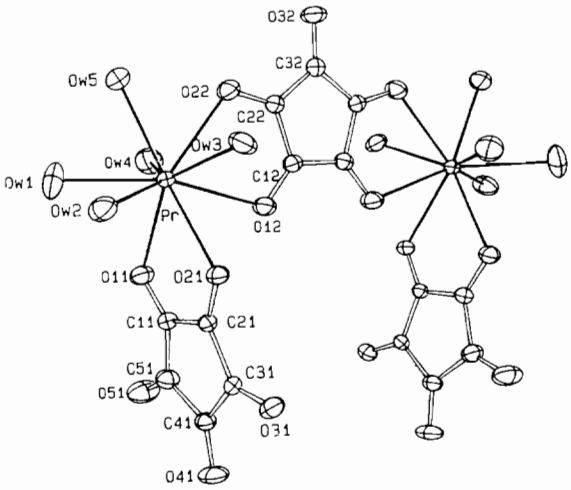

Fig. 1. View of the dinuclear entity, $[Pr(H_2O)_5]_2(C_5O_5)_3$, for the family **1**-Ln.

1-Ln: $[Pr(H_2O)_5]_2(C_5O_5)_3 \cdot 4H_2O$

The dinuclear entity (Fig. 1) is symmetrical around the twofold axis going through O32 and C32 atoms. The outstanding feature of this entity is the presence of a chelating croconate (CR1) and particularly of a bis-chelating one (CR2). As far as we are aware, the latter coordination mode has never been seen for this ligand; it will be discussed later. The central part of this entity (Pr and CR2) and the lateral one (Pr and CR1) make a dihedral angle of 83.0(2)°.

The praseodymium atom linked to four croconate oxygen atoms completes its environment by five water molecules: in general, croconate oxygen atoms are more distant from the praseodymium than water molecules (Table 5). The coordination polyhedron is close to a tricapped trigonal prism (Fig. 2); a dihedral angle of 6.0° is observed between the bases (Ow2, Ow3, Ow5 and O11, O12, Ow4).

TABLE 5. Interatomic distances (Å)[a] and bond angles (°) in $[Pr(H_2O)_5]_2(C_5O_5)_3 \cdot 4H_2O$

Around Pr			
Pr–Ow(1)	2.526(4)	Pr–O(11)	2.518(3)
Pr–Ow(2)	2.483(4)	Pr–O(21)	2.580(3)
Pr–Ow(3)	2.494(4)	Pr–O(12)	2.582(3)
Pr–Ow(4)	2.493(4)	Pr–O(22)	2.548(3)
Pr–Ow(5)	2.496(4)		
Croconate ligands		$i=1$	$i=2$
C(1i)–C(2i)		1.443(6)	1.457(6)
C(1i)–C(1i)^{i}			1.452(6)
C(2i)–C(3i)		1.445(5)	1.455(5)
C(3i)–C(4i)		1.483(6)	
C(4i)–C(5i)		1.475(6)	
C(5i)–C(1i)		1.462(6)	
C(1i)–O(1i)		1.243(5)	1.250(5)
C(2i)–O(2i)		1.264(4)	1.249(5)
C(3i)–O(3i)		1.241(5)	1.231(7)
C(4i)–O(4i)		1.227(5)	
C(5i)–O(5i)		1.221(6)	
O(1i)–C(1i)–C(2i)		122.7(3)	122.8(4)
O(1i)–C(1i)–C(1i)^{i}			129.8(4)
O(1i)–C(1i)–C(5i)		128.8(4)	
O(2i)–C(2i)–C(1i)		121.6(3)	122.8(4)
O(2i)–C(2i)–C(3i)		128.7(4)	127.7(4)
O(3i)–C(3i)–C(2i)		127.7(4)	126.9(2)
O(3i)–C(3i)–C(4i)		125.6(3)	
O(4i)–C(4i)–C(3i)		126.1(4)	
O(4i)–C(4i)–C(5i)		125.8(4)	
O(5i)–C(5i)–C(1i)		127.4(4)	
O(5i)–C(5i)–C(4i)		125.7(4)	
C(2i)–C(1i)–C(5i)		108.5(3)	
C(1i)^{i}–C(1i)–C(2i)			107.5(3)
C(1i)–C(2i)–C(3i)		109.7(3)	109.5(4)
C(2i)–C(3i)–C(4i)		106.7(3)	
C(2i)–C(3i)–C(2i)^{i}			106.1(4)
C(3i)–C(4i)–C(5i)		108.1(3)	
C(1i)–C(5i)–C(4i)		106.8(4)	
Hydrogen bonds and van der Waals contacts			
Intramolecular			
Ow(2)–Ow(6)	2.735(8)	Ow(2)–H(22)–Ow(6)	154.0(3)
Ow(1)–Ow(7)	2.74(1)		
O(11)–O(21)	2.777(5)		
O(12)–O(22)	2.810(4)		
Intermolecular			
Ow(1)–O(21)^{ii}	2.752(5)	Ow(1)–H(11)–O(21)^{ii}	177.9(4)
Ow(2)–O(41)^{iii}	2.756(5)	Ow(2)–H(12)–O(41)^{iii}	167.3(3)
Ow(3)–O(31)^{iv}	2.737(4)	Ow(3)–H(13)–O(31)^{iv}	150.3(2)
Ow(4)–O(51)^{v}	2.844(6)	Ow(4)–H(24)–O(51)^{v}	173.1(3)
Ow(5)–O(31)^{ii}	2.717(5)	Ow(5)–H(15)–O(31)^{ii}	154.1(2)
Ow(5)–Ow(8)^{vi}	2.90(1)	Ow(5)–H(25)–Ow(8)^{vi}	176.6(4)
Ow(4)–Ow(7)^{vii}	2.81(1)		
Ow(6)–Ow(7)^{viii}	2.72(1)		
Ow(6)–Ow(8)^{viii}	2.65(1)		
Ow(6)–O(32)^{ix}	2.704(7)		
Ow(6)–O(32)^{x}	2.704(7)		

[a]Code of equivalent positions: ^{i}: $\frac{3}{2}-x, \frac{1}{2}-y, z$; ^{ii}: $x-\frac{1}{2}, -y, \frac{1}{2}-z$; ^{iii}: $1-x, -y, -z$; ^{iv}: $\frac{3}{2}-x, y, \frac{1}{2}+z$; ^{v}: $x, \frac{1}{2}-y, \frac{1}{2}+z$; ^{vi}: $\frac{1}{2}-x, y, \frac{1}{2}+z$; ^{vii}: $\frac{1}{2}-x, \frac{1}{2}-y, z$; ^{viii}: $\frac{1}{2}+x, -y, \frac{1}{2}-z$; ^{ix}: $1-x, -y, 1-z$; ^{x}: $x-\frac{1}{2}, y-\frac{1}{2}, -z$.

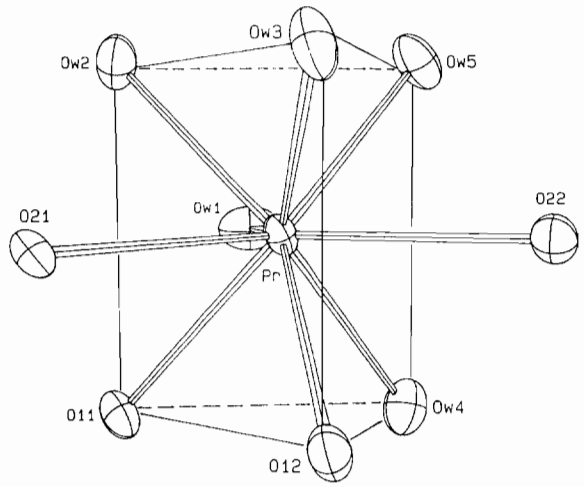

Fig. 2. Tricapped trigonal prism around praseodymium atom.

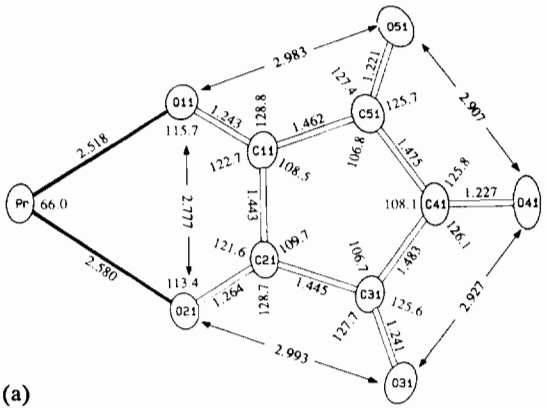

(a)

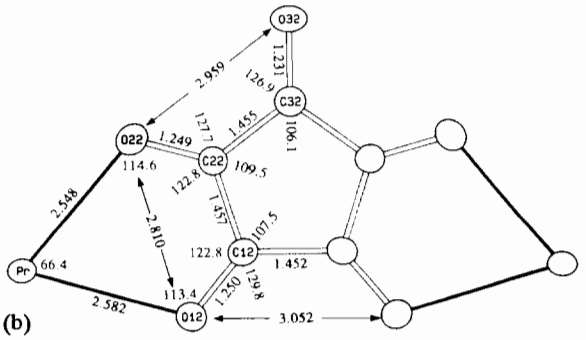

(b)

Fig. 3. The coordination mode of the croconate anions: CR1 (a), CR2 (b).

The chelation is more disymmetrical in the mono-chelating ligand (CR1), where the Pr–O distances inside the bite differ from $\Delta = 0.062$ Å, than in the bis-chelating ligand CR2, $\Delta = 0.034$ Å (Fig. 3) (Table 5). In previous structural studies, where the croconate ligand was mono-chelating Δ ranges from 0.003 to 0.34 Å [6, 7, 9, 26].

The chelation or bis-chelation effects involved some deformations of the cycles, which are more or less observable:

- the shortening of the distance O–O inside the bite with respect to the same distance outside the bite;
- O–C–C angles inside the bite more closed than angles outside the bite: O11–C11–C21 = 122.7(I3)° versus O11–C11–C51 = 128.8(4)°;
- C–C–C angles contiguous with the bite are generally more open than the respective angles outside the bite: C11–C21–C31 = 109.7(3)° versus C21–C31–C41 = 106.7(3)°;
- the lengthening of the C–O inside the bite as compared to the same distance outside the bite: C21–O21 = 1.264(4) Å versus C31–O31 = 1.241(5) Å.

A detailed analysis of the geometry of these cycles needs to take in account, besides the chelation or bischelation, all the strains of these ligands and particularly the hydrogen bonds. Except for the O11 atom, all the CR1 oxygen atoms are hydrogen bonded to the water molecules linked to the praseodymium, in various symmetry operations (Table 5).

The CR2 ligand, presenting C_{2v} symmetry, is quasiplanar, while in the CR1 anion atom deviations to the mean plane reach 0.055(7) Å (O41) and 0.054(7) Å (O51): such an effect might be attributed to the hydrogen bonding. In spite of some distortion in the bond lengths and angles of these rings, delocalization is retained, as in copper croconate [6]. The average bond distances (C–C = 1.462(6) Å for CR1, 1.455(6) Å for CR2; C–O = 1.239(5) Å for CR1, 1.243(6) Å for CR2) compare favorably with the corresponding values (C–C = 1.46 Å, C–O = 1.26 Å) in the free croconate anion which exhibits extensive delocalization [8].

The crystal structure comes from two factors: the hydrogen bonding already mentioned (Table 5) and the stacking between croconate planes according to the sequence ...CR1–CR1–CR2–CR1... (Fig. 4). Two CR1 ligands related by an inversion and a translation slightly overlap at the C31–O31 bond: the mean distance of this bond to the plane of the facing ligand is 3.37 Å. The C32–O32 bond is sandwiched between the two CR1 related by a twofold axis. The C32 atom is at a distance of 3.31 and 3.33 Å from the C41–O41 bonds of these two croconate ligands. Assuming that the C–C and C–O keep their double bond character (Table 5) such distances are indicative of van der Waals interactions. Such effects have been shown for the squarate ligand [27, 28].

Four $[Pr(H_2O)_5]_2(C_5O_5)_3 \cdot 4H_2O$ units are present in the cell. A projection view along the plane (100) is presented in Fig. 5. Besides the water molecules bonded to the praseodymium atom, free water molecules (Ow6, Ow7, Ow8) are also present: the two latter ones have 50% site occupancy. They are localized in three dimensional tunnels: bulkier tunnels occur along the [100] axis (Fig. 5). van der Waals interactions relate the free

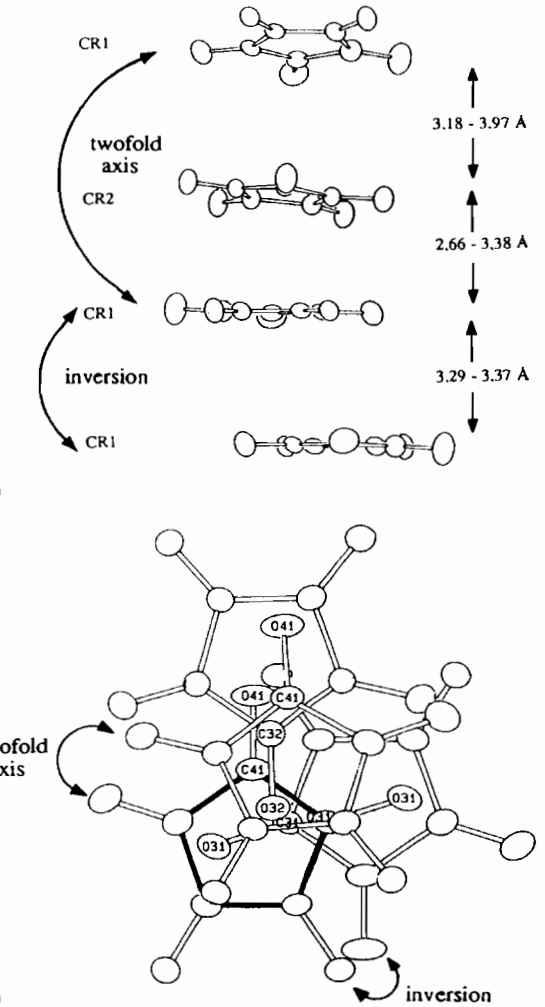

Fig. 4. The stacking of croconate anions: (a) side view, (b) projection on to the mean plane of CR1.

water molecules and the ones linked to the praseodymium atom.

2-Ln: $[Er(H_2O)_6]_2(C_5O_5)_3 \cdot 3H_2O$

This dinuclear entity is represented in Fig. 6; each entity contains two independent erbium atoms (Er1, Er2), three croconate ligands (CR1, CR2, CR3) and six water molecules per erbium atom. A dihedral angle of 3.3(8)° is observed between CR1 and CR2 and these two ligands make dihedral angles from CR3 of 13.1(6) and 12.4(4)°, respectively.

Each erbium atom is bound to eight oxygen atoms. Er–O bond lengths are homogeneous enough (between 2.244(9) and 2.38(1) Å, Table 6). No significant difference is observed between the Er1–O mean distance (2.34(1) Å) and that of Er2–O (2.33(1)Å). In both cases, the polyhedron geometry is closed to a square antiprism: dihedral angle values between the bases are 1.89° (Er1) and 4.47° (Er2) (Fig. 7). The evolution between the two families involves a modification of the

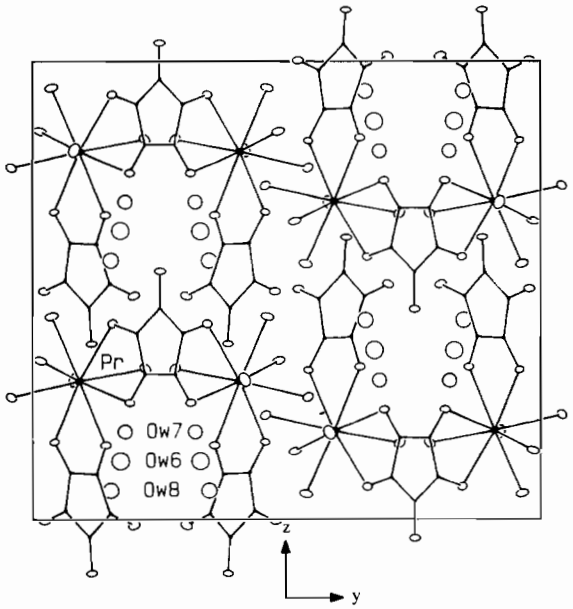

Fig. 5. View of the structure $[Pr(H_2O)_5]_2(C_5O_5)_3 \cdot 4H_2O$ down the *a* axis.

coordination number of the lanthanide from 9 (**1**-Ln) to 8 (**2**-Ln). Such a modification is consistent with the lanthanide contraction [19] and is likely to be due to steric effects [15, 27, 29].

The CR1 and CR2 ligands are monodentate (Fig. 6. C–C distances and C–C–C angles are similar for these two rings (Table 6). Some discrepancies are noted for the C–O distances as well as for the O–C–C angles. The C11–O11 bond length is among the largest while the C12–O12 is among the smallest (Table 6). The CR3 ligand is transmonodentate; its C–C distances vary from 1.44(1) to 1.49(1) Å and C–C–C angles range between 106.4(8) and 109.1(7)°. Interestingly, the oxygen atoms bound to the erbium atom (O13, O33) show the same C–O bond length (1.25(1) Å). The other C–O distances are smaller (Table 6). The five croconate carbons of these rings are nearly coplanar, within 0.03(1) Å (C43). Considering the whole ligand (carbon and oxygen atoms) these three cycles show significant deviations from planarity with atom distances to the mean planes reaching 0.142(7) Å (C41), 0.162(9) Å (O32) and 0.116(9) Å (O53). Moreover the angle sum towards C41 and C42 deviates from 360°; it reaches 356(2)° and 357(2)°, respectively. In addition to the coordination mode of these three ligands, the hydrogen bonding or van der Waals interactions between the croconate oxygen atoms and water molecules bound to erbium atom helps account for these deformations (Table 6).

The croconate planes are stacked according to the sequence ...CR1–CR2–CR3–CR1.... A projection onto the mean plane of CR2 shows a particular overlap of the bonds C51–C11 and C12–C52 (Fig. 8). C12 and C52 are at 3.37(1) and 3.19(1) Å from the C51–C11 bond, respectively. Many other atoms participate at this overlap: the average distance between the CR1 and CR2 planes is equal to 3.235(8) Å. An overlap also exists between the CR2 and CR3 ligands. The involved atoms for the CR3 ligand are C13, C23, C43, C53 and O43: their respective distance from the mean plane of CR2 ranges from 2.91(1) to 3.74(1) Å. As indicated above in the case of the family **1**-Ln, such distances are likely to result from some charge-transfer [28].

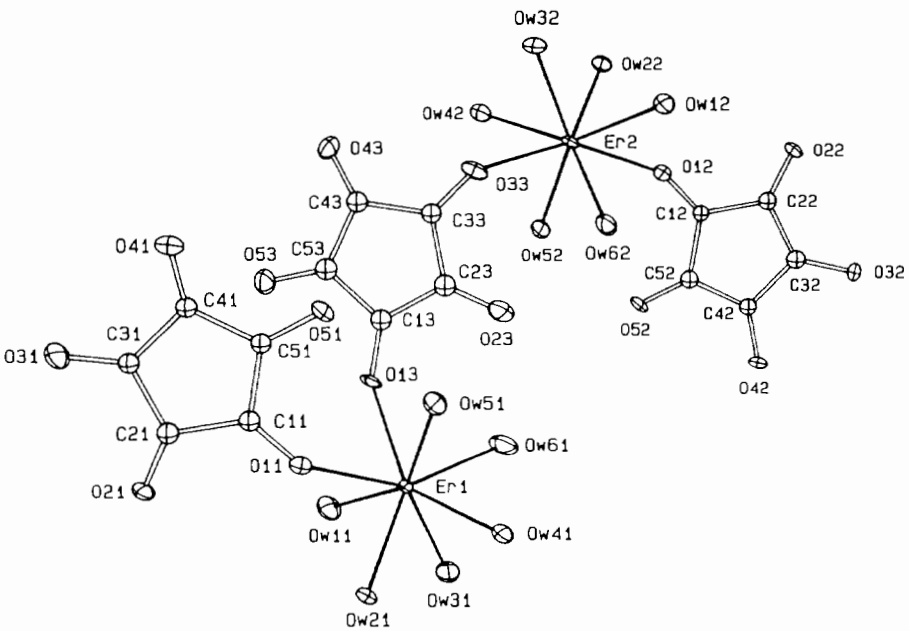

Fig. 6. View of the dinuclear entity, $[Er(H_2O)_6]_2(C_5O_5)_3$, for the family **2**-Ln.

TABLE 6. Interatomic distances (Å)[a] and bond angles (°) in $[Er(H_2O)_6]_2(C_5O_5)_3 \cdot 3H_2O$

Around Er	$i=1$	$i=2$	
Er(i)–O(1i)	2.28(1)	2.38(1)	
Er(i)–O(13)	2.353(8)		
Er(i)–O(33)		2.33(1)	
Er(i)–Ow(1i)	2.34(1)	2.35(1)	
Er(i)–Ow(2i)	2.37(1)	2.32(1)	
Er(i)–Ow(3i)	2.31(1)	2.38(1)	
Er(i)–Ow(4i)	2.38(1)	2.30(1)	
Er(i)–Ow(5i)	2.37(1)	2.244(9)	
Er(i)–Ow(6i)	2.35(1)	2.337(9)	
Croconate ligands	$i=1$	$i=2$	$i=3$
C(1i)–C(2i)	1.47(1)	1.47(1)	1.44(1)
C(2i)–C(3i)	1.47(1)	1.47(1)	1.46(1)
C(3i)–C(4i)	1.468(9)	1.468(9)	1.49(1)
C(4i)–C(5i)	1.47(1)	1.47(1)	1.46(1)
C(5i)–C(1i)	1.47(1)	1.47(1)	1.48(1)
C(1i)–O(1i)	1.27(1)	1.22(1)	1.25(1)
C(2i)–O(2i)	1.25(1)	1.24(1)	1.22(1)
C(3i)–O(3i)	1.25(1)	1.26(1)	1.25(1)
C(4i)–O(4i)	1.24(1)	1.27(1)	1.20(1)
C(5i)–O(5i)	1.26(1)	1.21(1)	1.23(1)
O(1i)–C(1i)–C(2i)	125.7(7)	124.1(7)	127.5(9)
O(1i)–C(1i)–C(5i)	125.3(7)	127.7(7)	123.5(9)
O(2i)–C(2i)–C(1i)	122.4(8)	127.9(8)	126.7(9)
O(2i)–C(2i)–C(3i)	128.9(8)	122.2(7)	125.2(9)
O(3i)–C(3i)–C(2i)	124.4(7)	126.6(7)	124.5(9)
O(3i)–C(3i)–C(4i)	126.2(8)	122.2(7)	126.3(9)
O(4i)–C(4i)–C(3i)	122.8(8)	124.9(7)	126.3(8)
O(4i)–C(4i)–C(5i)	125.3(7)	123.8(7)	127.2(9)
O(5i)–C(5i)–C(1i)	127.4(8)	125.6(8)	125.5(9)
O(5i)–C(5i)–C(4i)	124.6(8)	126.3(8)	126.7(9)
C(2i)–C(1i)–C(5i)	108.0(6)	108.0(6)	108.9(8)
C(1i)–C(2i)–C(3i)	108.0(6)	108.0(6)	107.6(9)
C(2i)–C(3i)–C(4i)	108.0(6)	108.0(6)	109.1(7)
C(3i)–C(4i)–C(5i)	108.0(6)	108.0(6)	106.4(8)
C(1i)–C(5i)–C(4i)	108.0(6)	108.0(6)	107.7(8)

Hydrogen bonds and van der Waals contacts

Intramolecular			
Ow(51)–O(51)	2.67(1)	Ow(51)–H(251)–O(51)	163.2(6)
Ow(61)–O(23)	2.70(1)	Ow(61)–H(161)–O(23)	158.4(7)
Ow(61)–Ow(10)	2.53(2)	Ow(61)–H(261)–Ow(10)	151.5(7)
Ow(52)–O(52)	2.73(1)	Ow(52)–H(252)–O(52)	167.1(6)
Ow(62)–O(23)	2.68(1)	Ow(62)–H(162)–O(23)	172.9(7)
Ow(11)–Ow(31)	2.72(1)		
Ow(11)–O(13)	2.80(1)		
Ow(21)–O(11)	2.69(1)		
Ow(21)–Ow(41)	2.74(1)		
Ow(31)–Ow(11)	2.72(1)		
Ow(31)–Ow(61)	2.76(1)		
Ow(41)–Ow(51)	2.72(1)		
Ow(51)–O(11)	2.79(1)		
Ow(12)–Ow(62)	2.67(1)		
Ow(12)–Ow(32)	2.78(1)		
Ow(22)–O(12)	2.70(1)		
Ow(22)–Ow(42)	2.76(1)		
Ow(32)–O(33)	2.78(1)		

(*continued*)

TABLE 6. (*continued*)

Hydrogen bonds and van der Waals contacts

Intramolecular			
Ow(42)–O(33)	2.68(1)		
Ow(42)–Ow(52)	2.80(1)		
Ow(62)–O(33)	2.81(1)		
Ow(9)–Ow(10)	2.54(2)		
Ow(10)–Ow(61)	2.53(2)		
Intermolecular			
Ow(11)–O(41)^{iii}	2.74(1)	Ow(11)–H(111)–O(41)^{iii}	173.3(7)
Ow(11)–Ow(9)^{i}	2.84(2)	Ow(11)–H(211)–Ow(9)^{i}	161.7(7)
Ow(21)–O(22)^{iv}	2.71(1)	Ow(21)–H(121)–O(22)^{iv}	179.2(7)
Ow(21)–Ow(22)^{iv}	2.85(1)	Ow(21)–H(221)–Ow(22)^{iv}	179.3(7)
Ow(31)–O(51)^{iii}	2.73(1)	Ow(31)–H(131)–O(51)^{iii}	162.2(7)
Ow(31)–Ow(7)^{iii}	2.78(1)	Ow(31)–H(231)–Ow(7)^{iii}	157.0(6)
Ow(41)–O(21)^{v}	2.78(1)	Ow(41)–H(141)–O(21)^{v}	171.4(7)
Ow(41)–Ow(8)^{ii}	2.57(1)	Ow(41)–H(241)–Ow(8)^{ii}	152.8(7)
Ow(51)–O(31)^{v}	2.71(1)	Ow(51)–H(151)–O(31)^{v}	173.7(7)
Ow(12)–O(42)^{vii}	2.66(1)	Ow(12)–H(112)–O(42)^{vii}	169.3(7)
Ow(12)–O(43)^{v}	2.78(1)	Ow(12)–H(112)–O(43)^{v}	135.4(6)
Ow(22)–O(21)^{viii}	2.72(1)	Ow(22)–H(122)–O(21)^{viii}	175.4(6)
Ow(22)–O(41)^{ix}	2.93(1)	Ow(22)–H(222)–O(41)^{ix}	147.9(6)
Ow(32)–O(52)^{vii}	2.76(1)	Ow(32)–H(132)–O(52)^{vii}	179.6(7)
Ow(32)–Ow(8)^{vii}	2.61(1)	Ow(32)–H(232)–Ow(8)^{vii}	164.0(7)
Ow(42)–O(22)^{i}	2.69(1)	Ow(42)–H(142)–O(22)^{i}	170.4(7)
Ow(42)–Ow(7)^{vi}	3.08(1)	Ow(42)–H(242)–Ow(7)^{vi}	175.5(7)
Ow(52)–O(32)^{i}	2.68(1)	Ow(52)–H(152)–O(32)^{i}	148.7(6)
Ow(62)–O(53)^{v}	2.76(1)	Ow(62)–H(262)–O(52)^{v}	179.3(5)
Ow(7)–Ow(10)^{vii}	2.00(1)		
Ow(7)–Ow(31)^{vii}	2.78(1)		
Ow(8)–Ow(41)^{vi}	2.57(1)		
Ow(8)–Ow(32)^{iii}	2.61(1)		
Ow(8)–O(32)^{i}	2.77(1)		

[a]Code of equivalent positions: ^{i}: $x-1, y, z$; ^{ii}: $x, y-1, z$; ^{iii}: $x, y, z-1$; ^{iv}: $x-1, y-1, z-1$; ^{v}: $x+1, y, z$; ^{vi}: $x, y+1, z$; ^{vii}: $x, y, z+1$; ^{viii}: $x+1, y+1, z+1$; ^{ix}: $x+1, y+1, z$.

The unit cell contains one entity $[Er(H_2O)_6]_2(C_5O_5)_3 \cdot 3H_2O$. The free water molecules (Ow7, Ow8, Ow9, Ow10) are localized into tunnels, the axes of which are parallel to the [001] direction (Fig. 9): the two latter water molecules have an occupation site of 50%. All the free water molecules contribute to the lattice cohesion.

Thermal behaviour

The complete dehydration of hydrated lanthanide croconates is a single-step process which takes place from 90 to 150 °C (Figs. 10 and 12). The amount of lost water fits rather well with the composition established by structural work or chemical analyses (Tables 7 and 8). An endotherm is shown for this process (Figs. 11 and 13). The anhydrous compounds were isolated and found to be amorphous. Plateaux corresponding to anhydrous compounds extend over a temperature range of about 100 ° to 200 °C. In this respect, the

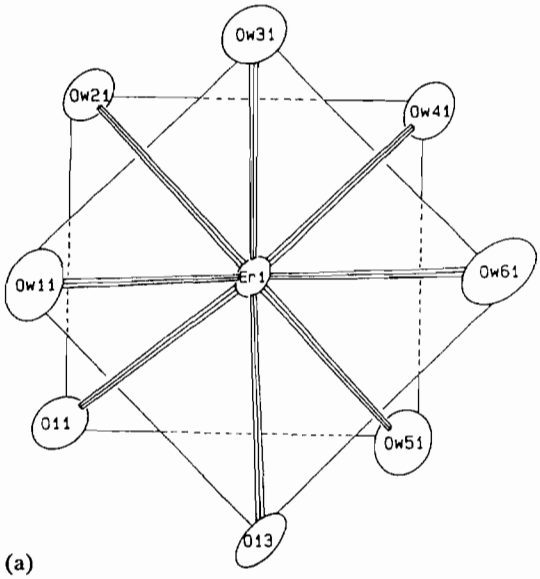

(a)

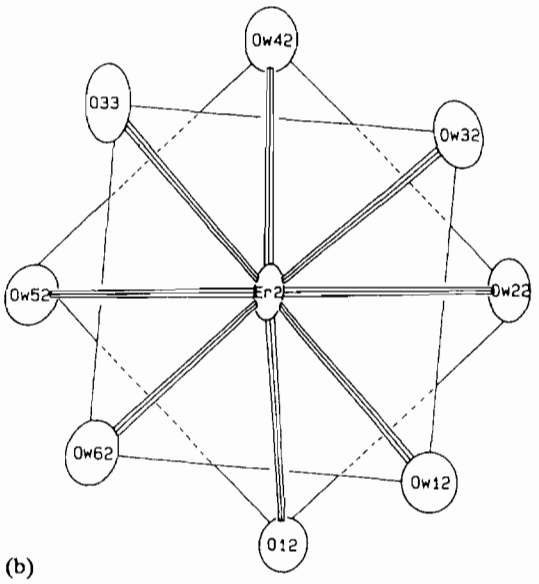

(b)

Fig. 7. Square antiprism around erbium atoms: Er1 (a), Er2 (b).

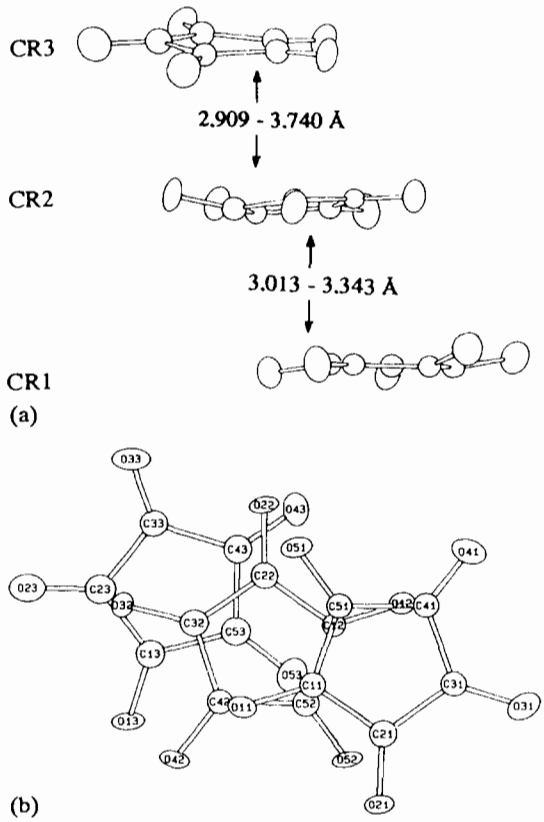

Fig. 8. The stacking of croconate anions: (a) side view, (b) projection on to the plane of CR2.

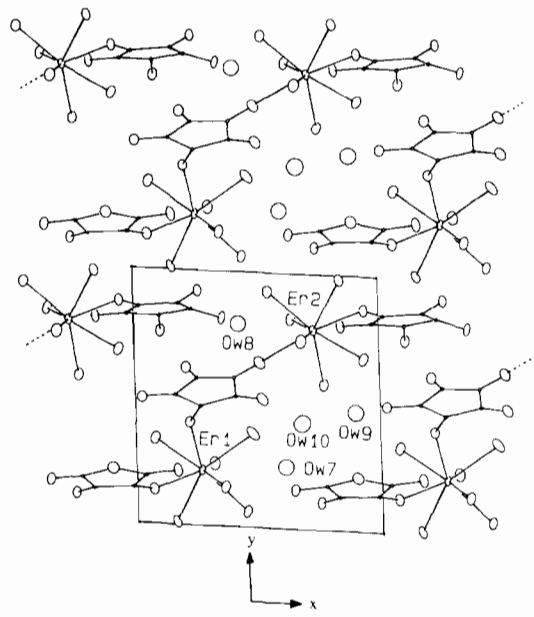

Fig. 9. View of the structure $[Er(H_2O)_6]_2(C_5O_5)_3 \cdot 4H_2O$ down the *c* axis.

lanthanide croconates resemble the thermal behaviour of lanthanide squarates [16].

The croconate ligand decomposition begins near 360 °C and extends over a wide temperature range. In several cases no final horizontal plateau is reached below 680 °C. With the conditions used, the decomposition process is exothermic (Figs. 11 and 13, Tables 7 and 8). The formation of oxycarbonate by croconate decomposition is more or less noticed according to the considered lanthanide (Figs. 10 and 12). Stable oxides are the final products.

For the cerium croconate (**1**-Ln) decomposition of the ligand is a single-step process which occurs in a very narrow temperature range between 310 and 330 °C (Fig. 10). Ceric oxide is obtained around 330 °C (Table 7). One single-step process corresponds to the decomposition of terbium croconate but a wide temperature range from 365 to 500 °C is necessary to get Tb_4O_7 (Fig. 12, Table 8).

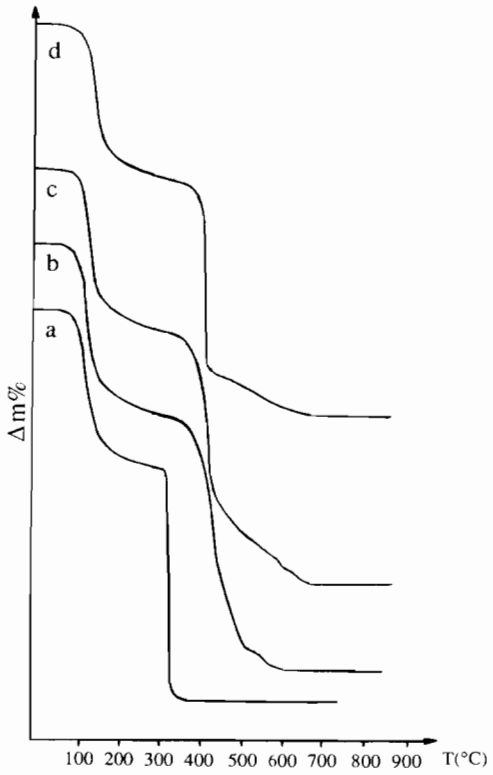

Fig. 10. TGA curves for 1-Ln compounds: (a) Ce, (b) Pr, (c) Sm, (d) Gd.

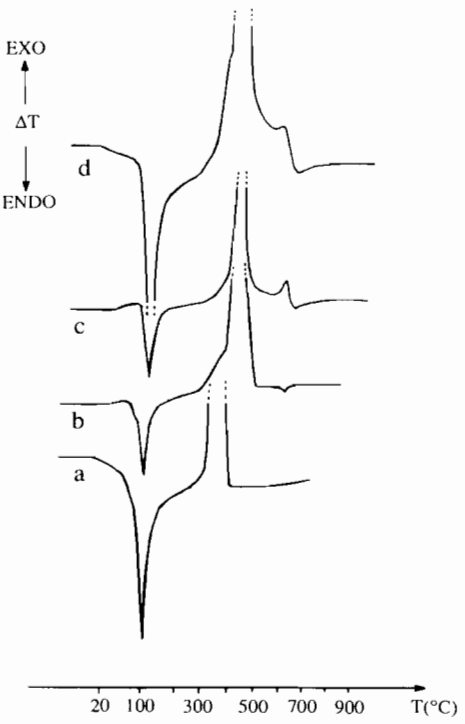

Fig. 11. DTA curves for 1-Ln compounds: (a) Ce, (b) Pr, (c) Sm, (d) Gd.

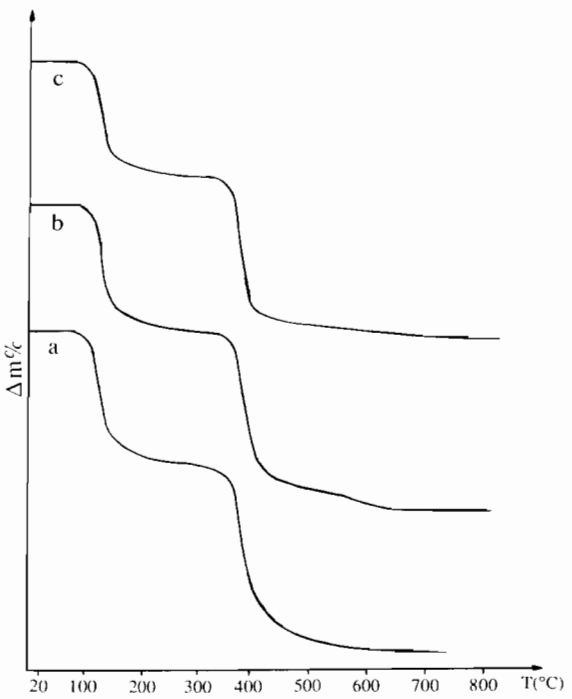

Fig. 12. TGA curves for 2-Ln compounds: (a) Tb, (b) Ho, (c) Yb.

For the other compounds of the first family, decomposition is at least a double stage process: first a steep slope with a singular point at 490 (Pr), 430 (Sm) and 395 (Gd) °C and then, except for Pr, a sluggish slope until constant weight is observed. For the Pr compound a pseudo-plateau is obtained between 490 and 530 °C whose composition corresponds to the oxycarbonate $Pr_2O_2CO_3$ [30] (Fig. 10). The decarbonation of this latter phase starts around 550 °C and terminates at 600 °C. For the sake of clarity, Nd or Eu compounds are not represented in Fig. 10, their decomposition is similar to that of the Sm compound. Weight losses indicate that the composition $Sm_2(CO_3)_3$ corresponds to the singular point at 430 °C, and $Gd_2O(CO_3)_2$ fits well with that at 395 °C. The latter phases lose their carbonate gradually as the temperature increases. This was not observed for the corresponding lanthanides squarates or oxalates [16, 31]. Srivastava and Vasudeva Murthy, observed the formation of stable oxycarbonates $La_2O((CO_3)_2$ [32], but this observation has been recently questioned [33]. A major exothermic peak is observed when the decomposition of the croconate takes place, but the basis of these peaks appears to be broad, and in several cases satellite peaks are involved.

For the second family the decomposition of croconate via oxycarbonate becomes noticeably less as the lanthanide ionic radius decreases [19]. This phenomenon was observed with the lanthanide squarates and oxalates [16, 31]. For sake of clarity the respective curves of Dy and Er croconate are not represented in Figs. 12

TABLE 7. Thermal decomposition of **1**-Ln family

	Dehydration weight loss (%)		DTA endotherm (°C)	Decomposition weight loss (%)		DTA exotherm (°C)
	calculated	observed		calculated	observed	
1-Ce	26.40	26.3	105	39.06	37.8	350
1-Pr	26.41	25.7	100	37.84	37.8	405
1-Nd	26.24	25.9	120	38.73	38.7	407
1-Sm	25.91	24.5	105	33.72	36.0	405
1-Eu	25.82	25.9	120	38.11	38.9	400
1-Gd	25.54	24.5	110	37.71	38.5	415

TABLE 8. Thermal decomposition of **2**-Ln family

	Dehydration weight loss (%)		DTA endotherm (°C)	Decomposition weight loss (%)		DTA exotherm (°C)
	calculated	observed		calculated	observed	
2-Tb	26.79	25.9	120	36.11	35.0	400
2-Dy	26.60	25.9	125	36.65	37.1	410
2-Ho	26.47	26.3	120	36.47	36.6	395
2-Er	26.37	26.7	125	36.33	36.2	405
2-Yb	26.06	25.9	135	35.91	35.2	395

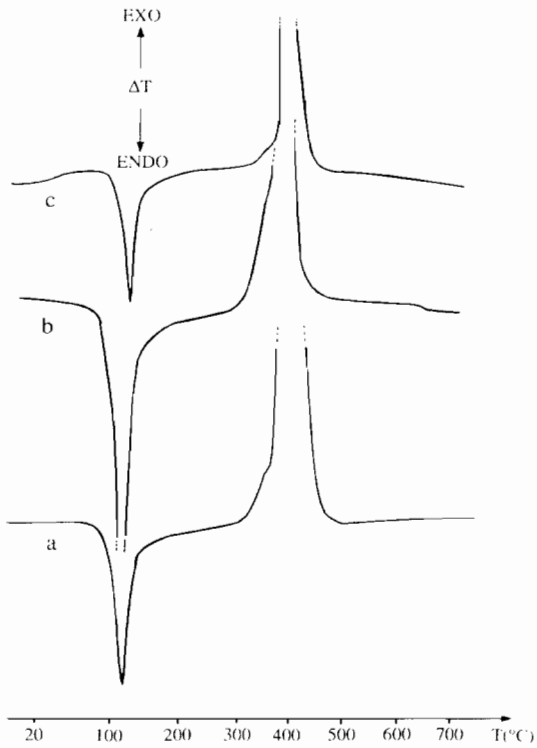

Fig. 13. DTA curves for **2**-Ln compounds: (a) Tb, (b) Ho, (c) Yb.

and 13 but they are very similar to the ones of Ho compound. A small weight loss at about 600 °C indicates that non-stoichiometric oxycarbonate is formed below that temperature for the holmium croconate. No oxycarbonate is observed for the decomposition of the ytterbium compound (Fig. 12).

Bottei *et al.* performed thermal studies of cobalt, nickel, copper and zinc croconates in an inert atmosphere [34]. Their results are very similar to the ones we obtained, but no oxycarbonate was observed. In an inert atmosphere the croconate decomposition displays a sharp exotherm [34].

Discussion

Previously the preparations of lanthanum, lutetium and yttrium croconates have failed with the conditions generally used in this kind of preparation. By reacting these elements, regardless of the counter-cation used (H^+, $(C_2H_5OH)_3NH^+$ and even K^+), the yellow solution of the croconate becomes progressively less and less yellow, colourless in approximately one week, eventually becoming a white scanty precipitate. For the other lanthanides (except the three quoted above) a faint modification of the colour of their croconate solution, at $pH \approx 4$, lasts from 20 days to one month.

For a long time croconic acid was shown to be reactive in the presence of reducing or oxidative agents [1, 3].

In 1958, Yamada *et al.* had indicated that croconic acid degraded in daylight, but they were unable to characterize the observed products [25]. Mesoxalic and oxalic acids were the products of oxidation of leuconic acid by a solution containing Mo(VI) in acidic medium [36]. Using ^{13}C NMR, croconic acid was shown to lead to mesoxalic and oxalic acid [26]. The factors involved

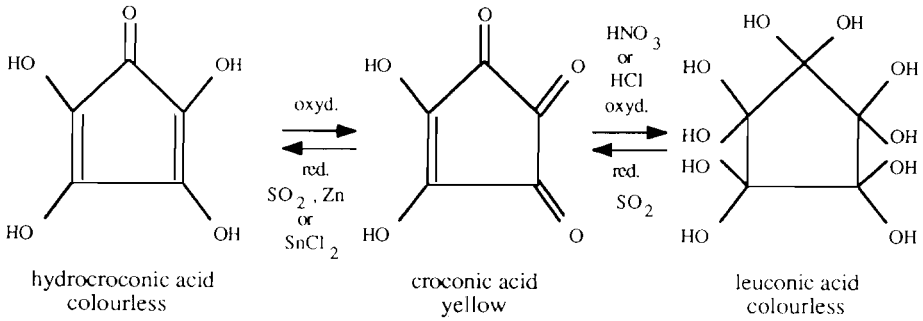

hydrocroconic acid
colourless

croconic acid
yellow

leuconic acid
colourless

were found to be not only daylight but also the presence of oxygen and the pH (the solution was buffered at different pH values) [26].

With the elements, lanthanum, lutetium and yttrium, in the three oxidation states, degradation occurs with croconic acid and also with the croconate solution (K^+, $(C_2H_5OH)_3NH^+$). We have given evidence that the factors leading to this phenomenon are pH, daylight and the presence of oxygen [17].

The more acidic the solution of the initial croconate, the shorter the time to obtain complete decoloration (from two days up to one week). In the case of croconic acid, acidified by a solution of HCl ($pH \approx 1$), single crystals of decahydrate lanthanum oxalate have been characterized. At pH values ranging from 1.5 to 4 the latter phase is still present but it is a minority one, as indicated by X-ray powder diffraction. The most abundant phase has not yet been identified.

Daylight and the presence of oxygen play a complementary role. A freshly prepared lanthanum croconate solution at $pH \approx 4$ ($(C_2H_5OH)_3NH^+$) is divided into two parts: one aliquot was in a vessel under vacuum in daylight, the other one was in a refrigerator (4 °C) in the presence of oxygen but in the absence of dalylight. After a month neither solution had become discolored.

The refrigerated solution formed yellow, tiny, single crystals. The chemical formula of this compound fitted with those of elements of the **1**-Ln family (Found: C, 19.10; H, 2.3. Calc.: C, 18.95; H, 2.95%) but its X-ray diagram could not be indexed on the basis of the **1**-Ln family. It is perhaps a temperature effect (4 versus 20 °C). Attempts to determine the structure of this compound have proved unsuccessful.

By starting with a refrigerated (4 °C) potassium croconate solution, a lanthanum phase isostructural with the cerium one, $CeK(H_2O)_7(C_5O_5)_2$, was obtained [18].

The three elements, La(III), Lu(III) and Y(III), hasten the degradation process of the croconate ligand. What is the difference between them and the whole lanthanide series? Two of these elements (La(III), Y(III)) have an electronic configuration of a rare gas, the third one, Lu(III), has a complete $4f^{14}$ electronic shell. As far as we are aware, it is the first time that the transition elements with a shell completely closed or empty distinguish themselves from elements with an incomplete electron shell. The precise mechanism of this distinction is not known.

The following experiment affords further proof of this distinction. A solution of triethanolammonium croconate is added to a solution containing both copper and lanthanum chloride (1/1). The first crystals recovered within three days are only the copper croconate according to their X-ray diagram. The second batch of brown–yellow micro-crystals recovered within a week corresponds to a mixture of copper croconate and lanthanum croconate: this latter phase was isostructural with the elements of the **1**-Ln family.

Why does the croconate ligand display a 1,2,4-coordination (1,2-chelation) towards the copper element and not towards the elements of the **2**-Ln family. A phenomenological theory, the 'bite angle' has been introduced to account for such behaviour [37]. The bite angle, *b*, is the ratio between the distance of two adjacent oxygen atoms of the ligand to the cation–oxygen distance inside the bite. The smaller *b* is, the greater is the possibility of a ligand–metal couple to be chelating; the upper value of *b* appears to be 1.52 [37]. For copper croconate, *b* is equal to 1.40 [6] while for erbium croconate (**2**-Ln) *b* is 1.26. A specific ligand may be chelating or non-chelating depending on the cation size [38]. However, the charge and environment of this cation must be taken into account [17].

When compared to the lanthanide squarates, this study of the previously unknown lanthanide croconates shows that the aqueous chemistry of the latter ligand is less constant than that of the former.

References

1 R. West, in R. West (ed.), *Oxocarbons*, Academic Press, New York, 1980, p. 1.
2 L. Gmelin, *Ann. Phys. (Leipzig, 4* (1825) 1.
3 R. West and J. Niu, in J. Zabicky (ed.), *The Chemistry of the Carbonyl Group*, Vol. 2, Interscience, London, 1970, Ch. 4, p. 241.

4 K. Yamada and Y. Hirata, *Bull. Chem. Soc. Jpn., 31*(5) (1958) 550.
5 R. West and H. Y. Niu, *J. Am. Chem. Soc., 85* (1963) 2586.
6 M. D. Glick, G. L. Downs and L. F. Dahl, *Inorg. Chem., 3*(12) (1964) 1712.
7 M. D. Glick and L. F. Dahl, *Inorg. Chem., 5*(2) (1966) 289.
8 N. C. Baenziger and J. J. Hegenbarth, *J. Am. Chem. Soc., 86* (1964) 3250.
9 Q. Chen, S. Liu and J. Zubieta, *Inorg. Chim. Acta, 175* (1990) 241.
10 D. Deguenon, G. Bernardinelli, J.-P. Tuchagues and P. Castan, *Inorg. Chem., 29* (1990) 3031.
11 D. Deguenon, P. Castan and F. Dahan, *Acta Crystallogr., Sect. C, 47* (1991) 433.
12 F. Maury, *Thèse de 3ième cycle,* Université Paul Sabatier, Toulouse, 1980.
13 C. Frasse, *Thèse de 3ième cycle,* Université Paul Sabatier, Toulouse, 1985.
14 A. Gleizes and M. Verdaguer, *J. Am. Chem. Soc., 106* (1984) 3727; M. Verdaguer, A. Gleizes, J.-P. Renard and J. Seiden, *Phys. Rev. B, 29* (1984) 5144.
15 J.-C. Trombe, A. Gleizes and J. Galy, *Inorg. Chim. Acta, 87* (1984) 129.
16 J.-F. Petit, *Thèse de Doctorat de l'Université,* Université Paul Sabatier, Toulouse, 1988.
17 C. Brouca-Cabarrecq, *Thèse de Doctorat de l'Université,* Université Paul Sabatier, Toulouse, 1991.
18 J.-C. Trombe and C. Brouca-Cabarrecq, *C. R. Acad. Sci., 310*(II) (1990) 521.
19 J. Flahaut, *Les Eléments des Terres Rares,* Masson, Paris, 1969.
20 C. Brouca-Cabarrecq and J.-C. Trombe, *C.R. Acad. Sci., 311*(II) (1990) 1179.
21 G. R. Choppin and E. Orebaugh, *Inorg. Chem., 17*(8) (1978) 2300.
22 A. C. T. North, D. C. Phillips and F. S. Mathews, *Acta Crystallogr., Sect. A, 24* (1968) 351.
23 *SDP Structure Determination Package,* Enraf-Nonius, Delft, 1979; C. K. Johnson, *ORTEP,* a Fortran thermal ellipsoid plot program for crystal structure illustrations, *Rep. ORNL-3974,* Oak-Ridge National Laboratory, TN, 1965.
24 *International Tables for X-ray Crystallography,* Vol. 4, Kynoch Press, Birmingham, UK, 1974, Tables 2.2A and 2.3.1.
25 A. Mosset, J. J. Bonnet and J. Galy, *Acta Crystallogr., Sect. B, 33* (1977) 2633.
26 E. D. Deguenon, *Thèse de Doctorat de l'Université,* Université Paul Sabatier, Toulouse, 1990.
27 J.-F. Petit, A. Gleizes and J.-C. Trombe, *Inorg. Chim. Acta, 167* (1990) 51.
28 W. M. Macintyre and M. S. Werkema, *J. Chem. Phys., 42* (1964) 3563.
29 E. Grenthe, Coll. Int. CNRS, *Les Eléments des Terres Rares,* CNRS éditeur, Paris, 1970, no. 180, 309.
30 R. P. Turcotte, J. O. Sawyer and L. Eyring, *Inorg. Chem., 8*(2) (1969) 238.
31 P. Pascal, *Nouveau Traité de Chimie Minérale,* Tome VII, Vol. 2, Masson Paris, 1959, p. 1003.
32 O. K. Srivastava and A. R. Vasudeva Murthy, *Curr. Sci. (India), 29* (1960) 470.
33 V. V. Subba Rao, R. V. G. Rao and A. B. Biswas, *J. Inorg. Nucl. Chem., 27* (1965) 2525.
34 R. S. Bottei, H. S. Chang and D. A. Lusardi, *J. Therm. Anal., 16* (1979) 389.
35 K. Yamada, N, Mizuno and Y. Hirata, *Bull. Chem. Soc. Jpn., 31* (1958) 543.
36 J. F. Verchère and M. B. Fleury, *Bull. Soc. Chim. Fr., 7* (1972) 2611.
37 D. L. Keppert, *Prog. Inorg. Chem., 23* (1977) 1.
38 X. Solans, M. Aguilo, A. Gleizes, J. Faus, M. Julve and M. Verdaguer, *Inorg. Chem., 29* (1990) 775.